Structure characterization and magnetic properties of oxide superlattices $La_{0.6}Sr_{0.4}MnO_3/La_{0.6}Sr_{0.4}FeO_3$

M. Izumi
Joint Research Center for Atom Technology (JRCAT), Tsukuba 305-0046, Japan

Y. Murakami
Photon Factory, Institute of Materials Structure Science, High Energy Accelerator Research Organization, Tsukuba 305-0801, Japan

Y. Konishi and T. Manako
Joint Research Center for Atom Technology (JRCAT), Tsukuba 305-0046, Japan

M. Kawasaki
Joint Research Center for Atom Technology (JRCAT), Tsukuba 305-0046, Japan
and Department of Innovative and Engineered Materials, Tokyo Institute of Technology, Yokohama 226-8502, Japan

Y. Tokura
Joint Research Center for Atom Technology (JRCAT), Tsukuba 305-0046, Japan
and Department of Applied Physics, University of Tokyo, Tokyo 113-8656, Japan
(Received 16 November 1998; revised manuscript received 8 February 1999)

Oxide superlattices composed alternatively of ferromagnetic metal layers of $La_{0.6}Sr_{0.4}MnO_3$ and antiferromagnetic insulator layers of $La_{0.6}Sr_{0.4}FeO_3$ were fabricated on $SrTiO_3$ substrates by pulsed laser deposition with controlling each layer thickness on an atomic scale. The near-perfect superlattice structure with atomically flat interfaces was verified by multiple peaks from Laue function in x-ray diffraction patterns with use of synchrotron radiation. An increase of antiferromagnetic $La_{0.6}Sr_{0.4}FeO_3$ layer thickness from 2 to 5 unit cells induces strong magnetic frustration around the superlattice interfaces, leading to reduction in magnetic transition temperature and ferromagnetic volume, while increasing the resistivity and magnetoresistance at low temperatures. [S0163-1829(99)15025-2]

Perovskites of transition metal oxides are quite suitable for fabrication of the artificial superlattice structure composed of ultrathin films with different compositions because of its chemical stability as well as the almost common lattice spacing. Making use of, for example, the carrier confinement effect, specific magnetic interaction at the interface, and some lattice strain effect, such a tailor-made material system based on the perovskite superlattice may open a new field of materials physics. For example, $KTaO_3/KNbO_3$ superlattices containing paraelectric and ferroelectric layers were demonstrated to show higher ferroelectric transition temperature than that of bulk $KNbO_3$,[1] superlattices composed of antiferromagnetic layers of $LaFeO_3$ and $LaCrO_3$ showed a ferromagnetic behavior,[2] and $DyBa_2Cu_3O_7/Sr_{1-x}Ca_xRuO_3$ superlattices were fabricated to study vortex dynamics in superconducting layers sandwiched with ferromagnetic layers.[3] Here, we fabricated oxide perovskite superlattices composed of ferromagnetic metal/antiferromagnetic insulator, $La_{0.6}Sr_{0.4}MnO_3/La_{0.6}Sr_{0.4}FeO_3$, to explore new magnetoelectronic properties.

$La_{1-x}Sr_xMnO_3$ is a prototypical half metal (i.e., 100% spin polarization in the ground state) having rather high Curie temperature, T_C, of 360 K.[4] By combining $La_{1-x}Sr_xMnO_3$ with other perovskite compounds in a form of superlattice, we can control new artificial degrees of freedom other than bandwidth or doping level. In this study, we have chosen an antiferromagnetic insulator, $La_{0.6}Sr_{0.4}FeO_3$ (LSFO), as another constituent layer to be combined with a ferromagnetic layer of $La_{0.6}Sr_{0.4}MnO_3$ (LSMO) to explore new magnetoelectronic properties arising from the competition between the magnetic ordering structures. The choice of doping level at $x=0.4$ in the LSFO layer, namely, 40% Sr^{2+} substitution on La^{3+} sites, comes from twofold reasons. The doping makes antiferromagnetic interaction weaker as indicated by the decrease of the Néel temperature from $T_N=700$ K for undoped $LaFeO_3$ to 320 K for doped LSFO, which is comparable with $T_C=310$ K for LSMO thin films.[5,6] Furthermore, the common *A*-site composition ($La_{0.6}Sr_{0.4}$) in constituent perovskite layers enables us to forget the surface terminating atomic layer problem during making heterointerfaces,[7] because MnO_2 and FeO_2 atomic layers are to be assembled in the *A*-O atomic layers without compositional modulation. We have already optimized the growth condition for the pulsed laser deposition of high-quality epitaxial $La_{0.6}Sr_{0.4}MnO_3$ thin films on $SrTiO_3$ (001) substrate.[7] The thickness can be controlled on an atomic scale by *in situ* monitoring of the intensity oscillation of reflection high energy electron diffraction (RHEED). The surface morphology is represented by 0.4 nm height steps and atomically flat terraces even when the film is as thick as 100 nm.

LSMO/LSFO superlattices were fabricated by pulsed laser deposition onto $SrTiO_3$ (001) single crystal substrates which were etched by a buffered fluoric acid.[8] The thickness

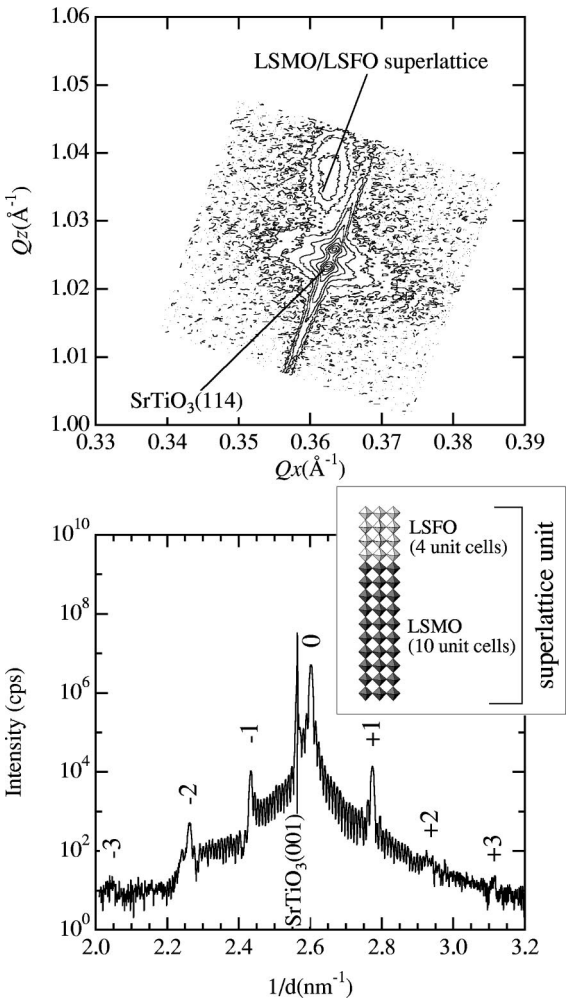

FIG. 1. Upper panel: Logarithmic contour plot around (114) diffraction for an $[(\mathrm{LSMO})10\ \mathrm{u.c.}/(\mathrm{LSFO})4\ \mathrm{u.c.}]_{20}$ superlattice. LSMO and LSFO stand for $La_{0.6}Sr_{0.4}MnO_3$ and $La_{0.6}Sr_{0.4}FeO_3$, respectively. Cu $K\alpha$ radiation was used. Q_x and Q_z correspond to [110] and [001] directions, respectively. In-plane lattice parameter for the superlattice estimated as $a=\sqrt{2}/Q_x$ is identical to that of the substrate, indicating coherent epitaxy. Lower panel: SRXRD pattern for an [(LSMO)10 u.c./(LSFO)4 u.c.] superlattice. The wavelength of SR was fixed at the absorption edge of Mn, 0.189 87 nm. The scattering direction was fixed at $[00l]$ direction. The satellite peaks are assigned to the lth superstructure peaks. Inset: A scheme of superlattice unit cell.

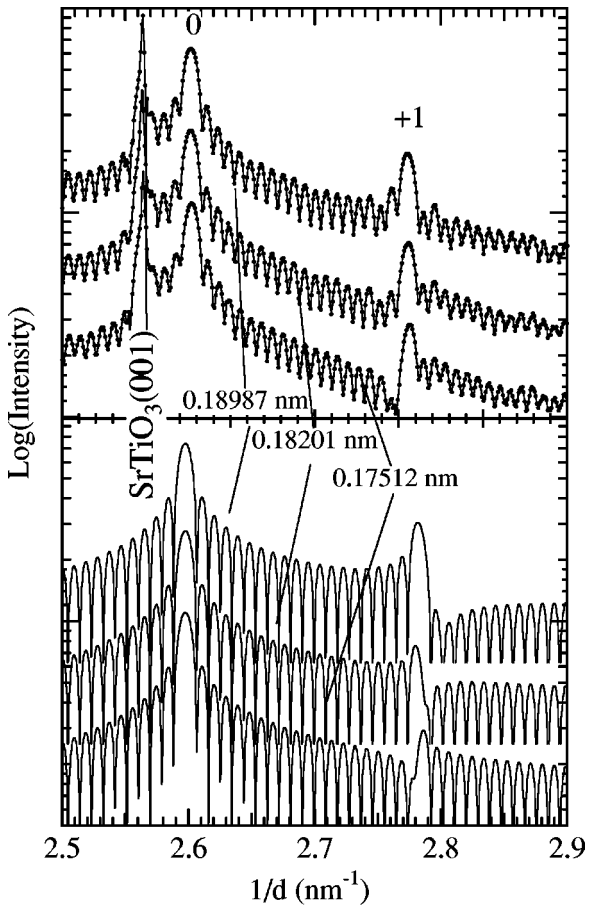

FIG. 2. Experimental (upper panel) and calculated (lower panel) SRXRD patterns for an $[(\mathrm{LSMO})10\ \mathrm{u.c.}/(\mathrm{LSFO})4\ \mathrm{u.c.}]_{20}$ superlattice on $SrTiO_3$ (001) with various wavelengths: 0.175 12 nm (Fe absorption edge), 0.189 87 nm (Mn absorption edge), and 0.182 01 nm (off-resonant position). The calculation was done using the one-dimensional step model, in which abrupt interface and ideally homogeneous distribution of layer thickness are assumed (see text).

of each LSMO layer was fixed at 10 unit cells (u.c.), whereas that of the LSFO layer was varied from 2 u.c. to 5 u.c. The growth condition of superlattices was identical to that reported previously for LSMO thin film deposition.[7] Synchrotron radiation x-ray diffraction (SRXRD) measurement was performed at the Photon Factory, KEK. The surface morphology was analyzed by an atomic force microscope (AFM). Magnetization was measured by a superconducting quantum interference device magnetometer. Magnetoresistance was measured by a conventional four probe method.

Prior to the superlattice experiment, we fabricated 100 nm thick LSFO thin films under the same deposition condition. The surface showed an atomically flat step-and-terrace structure in the observation of AFM. The crystal symmetry of the thin film is tetragonal with the identical in-plane lattice constant with that of $SrTiO_3$, and out-of-plane lattice constant of 0.390 nm, as verified by four-circle XRD. Resistivity at room temperature was 0.08 Ω cm and increased almost exponentially with lowering the temperature to 100 Ω cm at 210 K. There was no detectable magnetoresistance in this temperature range. From the temperature dependence of magnetization, T_N was estimated to be 250 K.

During the deposition of superlattices, clear RHEED intensity oscillation was observed routinely. Surface morphology of superlattices was also very smooth as examined by AFM images which showed 0.4 nm height steps corresponding to the unit cell height of perovskite. These results indicate that not only the surface but also the interfaces are atomically flat.

We first carried out off-axial XRD measurements around the (114) diffraction by using a four-circle diffractometer with a Cu $K\alpha$ source. The upper panel of Fig. 1 shows the reciprocal lattice mapping for an $[(\mathrm{LSMO})10\ \mathrm{u.c.}/(\mathrm{LSFO})4\ \mathrm{u.c.}]_{20}$ superlattice. The same Q_x values for the substrate and superlattice indicate that the in-plane lattice constant of the superlattice is expanded to fit that of the substrate. Since $SrTiO_3$ has a cubic crystal symmetry, the crystal structure of the superlattice is modified to the tetragonal one to keep the coherency at the interfaces in the superlattice.

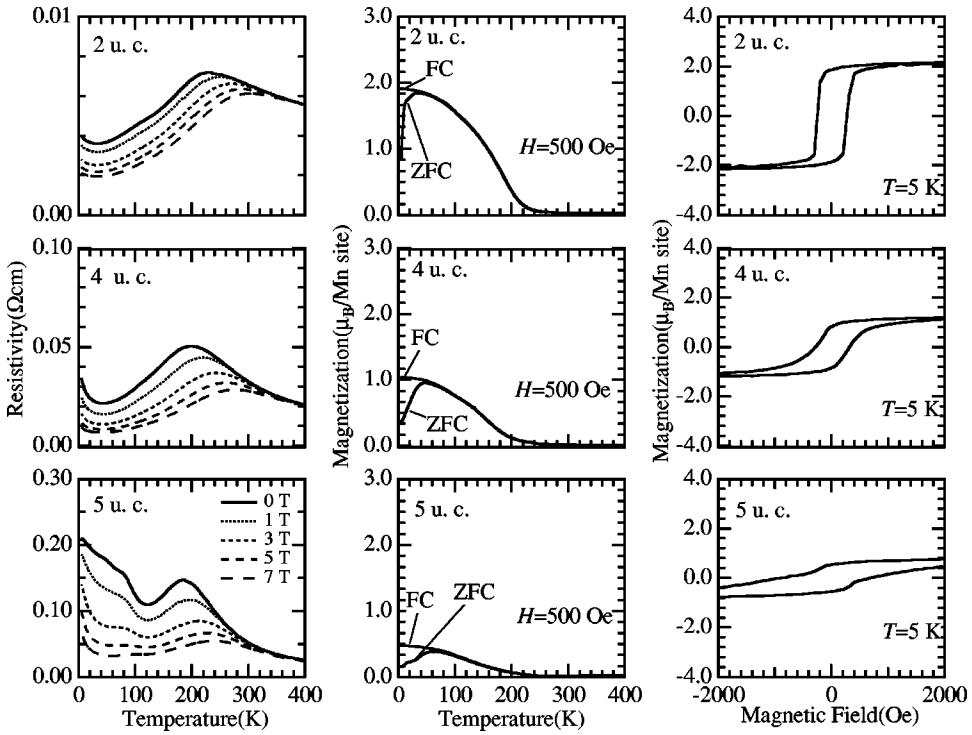

FIG. 3. Temperature dependence of resistivity (left panels), temperature dependence of magnetization at 500 Oe (middle panels), and magnetic field dependence of magnetization (right panels). LSFO thickness is 2 u.c. (top panels), 3 u.c. (middle panels), and 5 u.c. (bottom panels), while the thickness of the LSMO layer was fixed at 10 u.c. Resistance was measured along the [100] direction in the cubic setting. Resistivity was evaluated by assuming that only LSMO layers are conductive. Magnetic fields were applied along the [100]. Measurements of temperature dependence of magnetization were performed during warming after zero-field cooling as well as during cooling in magnetic field with the magnetic field of 500 Oe applied along the [100] direction. *M-H* curves were measured at 5 K after ZFC.

Weak satellite peaks originating from the superlattice periodicity were barely observed between the fundamental perovskite peaks along the $[00l]$ direction in XRD measurement. LSMO and LSFO have the same perovskite structure and there is a little difference in lattice parameters between them.[4,6] In addition, atomic scattering factor of Fe is very close to that of Mn. Therefore, to obtain detailed information, we carried out SRXRD studies. SR provides us not only with very brilliant x-ray but also with tunability of the wavelength. When the wavelength is fixed at an absorption edge of a constituent element, the relevant atomic scattering factor largely changes. Corrected atomic scattering factor f is given as

$$f = f^0 + \Delta f' + i\Delta f'', \tag{1}$$

where $\Delta f'$ and $\Delta f''$ are real and imaginary parts of the anomalous scattering factor, respectively.[9] As shown in the lower panel of Fig. 1, clear and sharp satellite peaks (denoted as $\pm 3, \pm 2, \pm 1$) show up around the fundamental peak of perovskite (denoted as 0).

We also compared the wavelength dependence of XRD patterns with calculations. The upper panel of Fig. 2 shows XRD patterns between the fundamental peak and $+1$ satellite peak measured at various wavelengths. Although all the measurements show similar results, the envelope of multiple peaks near the $+1$ superlattice peak shows appreciable difference depending on the wavelength. The lower panel of Fig. 2 shows calculated results using the following one-dimensional step model. The structure factor $F(K)$ of the superlattice as a function of scattering vector K is given as,[10]

$$F(K) = F_{\mathrm{LSMO}}(K)\sum_{s=0}^{m-1} \exp(iKsd_{\mathrm{LSMO}}) + F_{\mathrm{LSFO}}(K)\exp(iKmd_{\mathrm{LSMO}})\sum_{s=0}^{n-1} \exp(iKsd_{\mathrm{LSFO}}), \tag{2}$$

where m and n are layer numbers of LSMO and LSFO, respectively. d is the unit cell length along the $[00l]$ direction evaluated from XRD results for single-component thin films; $d_{\mathrm{LSMO}} = 0.383$ nm and $d_{\mathrm{LSFO}} = 0.390$ nm. $F(K)$ for each compound is calculated using atomic scattering factors f_{Mn} and f_{Fe} given by Eq. (1). The diffraction intensity $I(K)$ is given by

$$I(K) = I_e F^2(K) L(K), \tag{3}$$

where I_e and $L(K)$ are the Thomson factor and Laue function, respectively. When repetition p of the superlattice unit is small enough, $p-2$ submaximum peaks should appear due to the Laue function. As shown in Fig. 2, an excellent agreement between the observed and calculated results can be obtained, including the envelope shape of Laue function peaks near the $+1$ superlattice peak. The one-dimensional step model is based on the assumption that the thicknesses of alternating layers are well defined and that the interface is atomically flat and rigid. Therefore, we can conclude that the

fluctuation of thickness and the interdiffusion between Mn and Fe are small enough to be ignored.

Let us proceed to magnetic and electronic properties of the superlattices. We concentrate on three samples composed of ferromagnetic LSMO layers with the common thickness of 10 u.c. and antiferromagnetic LSFO layers with various thicknesses of 2, 4, and 5 u.c. The resistivity shown in the left panels of Fig. 3 was evaluated by assuming that the current flows only in the LSMO layers, since the resistivity of LSFO in this temperature range is orders of magnitude higher than that of LSMO. The T_C of the superlattice evaluated from the resistivity maximum decreases as 220 K, 200 K, and 185 K with increasing the LSFO layer thickness as 2 u.c., 4 u.c., and 5 u.c., respectively. In addition, the resistivity value itself also increases significantly and large magnetoresistance tends to subsist down to low temperatures with increase of the LSFO thickness. The results are obviously different from those of LSMO bulk crystals, which show T_C of 350–360 K and negligibly small magnetoresistance at low temperatures far below T_C.[4] The T_C of thick (>10 nm) epitaxial LSMO film on $SrTiO_3$ (001) is reduced to 310 K because of coherent strain induced from substrate as previously reported.[7] However, T_C's of superlattices are much lower than that of LSMO single-component thin film and they depend on the LSFO layer thickness even without changing thickness of the conductive LSMO layer (10 u.c.). Thus, the antiferromagnetic interaction of LSFO should strongly influence the magnetic properties of the LSMO layers, perhaps via the magnetic interaction through the interfaces.

The middle panels of Fig. 3 show temperature dependence of magnetization. Since the magnetic moment of the antiferromagnetic LSFO layers is expected to be small, the magnetization is assumed to originate from the LSMO layers alone and tentatively displayed as a quantity per Mn site. Significant difference between the samples is seen not only in the onset temperatures, which are consistent with T_C's obtained from the results of resistivity, but also in the magnitude of magnetization for field cooling (FC) at low temperature. The magnetic hysteresis curves measured at 5 K after zero-field cooling (ZFC) are shown in the right panels of Fig. 3. Coercive force (H_C) increases from 250 Oe to 1000 Oe as increasing the LSFO thickness from 2 u.c. to 5 u.c. The large H_C as observed is the origin of thermal hysteresis between FC and ZFC measurements.

On the basis of these transport and magnetic properties, the LSMO layer is considered to change gradually from a ferromagnetic metal to an antiferromagnetic insulator as increasing the thickness of the adjacent LSFO layers. Antiferromagnetically ordered spins of bulk LSFO direct along [111] in the simple cubic setting.[5,6] Thus it is anticipated that the square lattice of LSFO (001) plane at the interface between alternating layers contains antiparallel spin ordering along [110] direction. Therefore, strong frustration of spin arrangement should be produced at the LSMO/LSFO interfaces. According to preliminary results of Monte Carlo simulation on the classical spin model, the spin moment of LSFO layer aligns in the direction which is almost perpendicular to the net LSMO moment.[11] The originally ferromagnetically ordered spin moments of the LSMO layer cant alternatively

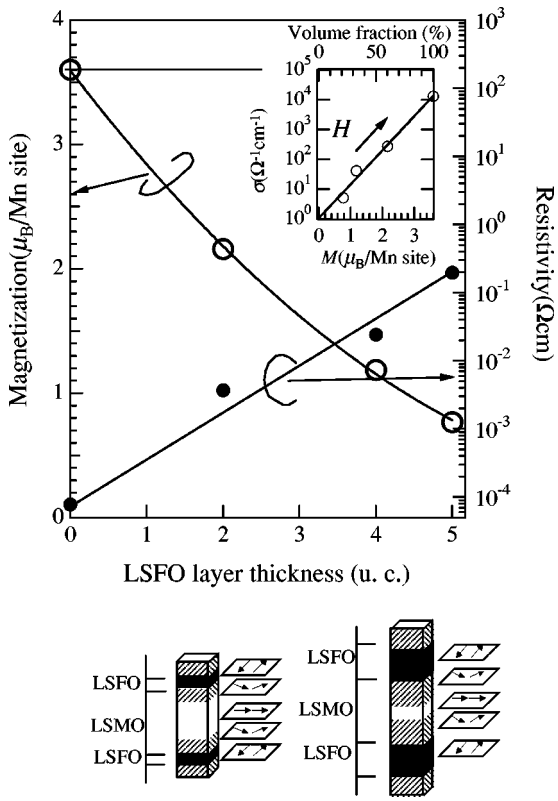

FIG. 4. Magnetization and resistivity of the superlattices, $[(\mathrm{LSMO})10\ \mathrm{u.c.}/(\mathrm{LSFO})n\ \mathrm{u.c.}(n=0, 2, 4, \text{and } 5)]_{20}$, as a function of LSFO layer thickness. Magnetization was obtained by *M*-*H* curve measurements at 5 K and 2000 Oe. Resistivity was measured at 20 K along the [100] direction in the simple cubic setting without applying magnetic field. Figures shown in lower panel are schematic illustrations of the superlattices. LSFO layers are shown as black areas. Hatched areas indicate spin-canting region due to the existence of antiferromagnetic interaction at the interfaces. The volume of the spin-canting region increases with increasing the LSFO layer thickness. Inset: Plot of conductivity versus magnetization. Volume fraction in the upper abscissa means the magnetization of superlattices divided by $3.6\mu_B$ which is saturation magnetization of fully ferromagnetic LSMO single layer film.

at the interface, corresponding to the antiferromagnetic ordering of LSFO in the film plane.

To substantiate the above picture, we show in Fig. 4 the magnetization and resistivity of the superlattices as a function of LSFO layer thickness. Since the observed magnetization is presented as per Mn site, the decrease of magnetization is due to the antiferromagnetic order or spin canting of the originally ferromagnetic LSMO layer at the interface. The increase of LSFO layer thickness makes the ferromagnetic volume fraction small as represented by the change in the magnetization (M) value (open circle) and also shown in the schematic illustration in the lower panel of Fig. 4. Therefore, the robustness of the antiferromagnetic spin structures in the LSFO and effective penetration depth of spin canting region of the LSMO layer may depend on the thickness of the LSFO layers in the superlattice structure. Such a change in magnetic coupling seems to be reflected in charge transport in the LSMO layers. The inset to Fig. 4 shows the relation between M and conductivity (σ) at a low temperature (20 K): Logσ is almost proportional to M, namely, the con-

ductivity increases exponentially with the effective thickness of the ferromagnetic layers. Magnetic field can increase the magnetization of superlattices gradually as a result of reducing the volume of the antiferromagnetic or spin canting region, and hence increase conductivity via an increase of ferromagnetic volume fraction of LSMO layer. This can explain the observed large magnetoresistance at temperatures enough lower than T_C.

In summary, we have fabricated high-quality coherent LSMO/LSFO superlattices. XRD measurements indicated that the superlattices have a well-defined superlattice structure on an atomic scale. With increasing thickness of the antiferromagnetic LSFO layer, T_C and magnetization at low temperature are lower. Weakening of ferromagnetism also makes resistivity higher and insulating, but in turn, enhances the magnetoresistance down to low temperature. These results indicate that antiferromagnetic spin arrangement in the LSFO layer modifies the ferromagnetic spin arrangement of the LSMO layer via the frustrated magnetic interaction at the interfaces. The effective strength of antiferromagnetic interaction caused by the LSFO layer seems to depend on its layer thickness.

We are grateful to N. Nagaosa and R. Maezono for stimulating discussions and for informing us of the Monte Carlo result prior to publication. This work, partly supported by New Energy and Industrial Technology Development Organization (NEDO) of Japan, was performed in the JRCAT under the joint research agreement between the National Institute for Advanced Interdisciplinary Research (NAIR) and the Angstrom Technology Partnership (ATP).

[1] H.-M. Christen, L.A. Boatner, J.D. Budai, M.F. Chisholm, L.A. Gea, P.J. Marrero, and D.P. Norton, Appl. Phys. Lett. **68**, 1488 (1996); E.D. Specht, H.-M. Christen, D.P. Norton, and L.A. Boatner, Phys. Rev. Lett. **80**, 4317 (1998).

[2] K. Ueda, H. Tabata, and T. Kawai, Science **280**, 1064 (1998).

[3] L. Miéville, E. Koller, J.-M. Triscone, M. Decroux, Ø. Fischer, and E.J. Williams, Phys. Rev. B **54**, 9525 (1996).

[4] A. Urushibara, Y. Moritomo, T. Arima, A. Asamitsu, G. Kido, and Y. Tokura, Phys. Rev. B **51**, 14 103 (1995).

[5] W.C. Koehler and E.O. Wollan, J. Phys. Chem. Solids **2**, 100 (1957).

[6] S. K. Park, T. Ishikawa, and Y. Tokura (unpublished).

[7] M. Izumi, Y. Konishi, T. Nishihara, S. Hayashi, M. Shinohara, M. Kawasaki, and Y. Tokura, Appl. Phys. Lett. **73**, 2497 (1998).

[8] M. Kawasaki, K. Takahashi, T. Maeda, R. Tsuchiya, M. Shinohara, T. Yonezawa, O. Ishihara, M. Yoshimoto, and H. Koinuma, Science **266**, 1540 (1994).

[9] *International Tables for Crystallography*, edited by T. Hahn (Kluwer Academic Publishers, Boston, 1995).

[10] *Metallic Superlattices*, edited by T. Shinjo and T. Takada (Elsevier, Amsterdam 1987).

[11] N. Nagaosa and R. Maezono (private communication).